

Aging Effects of an Elastic String Diffusing in a Disordered Media

Hajime Yoshino

Institute for Solid State Physics, the Univ. of Tokyo, 7-22-1 Roppongi, Minato-ku, Tokyo 106-8666 Japan

The aging effects of a 'diffusing glass', a single elastic string diffusing in a two-dimensional disordered media assisted by thermal noise are studied by Monte Carlo (MC) simulations. We find for the first time convincing numerical evidence of non-trivial aging effects both in the linear response against transverse force and the associated correlation function. Our results retain some important predictions of the conventional dynamical mean-field theory (MFT) but also reveal remarkable differences from it.

PACS numbers: 74.60.Ge, 02.50.Ey, 75.50.Lk

Elastic objects diffusing in disordered media assisted by thermal noise, which we call simply as 'diffusing glasses', are expected to remain persistently *non-stationary* due to the complicated competitions between the elasticity and disorder. An example will be a single vortex line diffusing in a type-II super-conductor with randomly distributed pinning centers. A dynamical MFT of elastic manifolds in random media [1] has been developed which proposes a self-consistent picture for such dynamics and predicts existence of aging effects similar to those found in spin-glasses. [2] However, the MFT is exact only in infinite dimensional embedding space. Compared with many *driven* dynamics [3] of the same elastic objects, much less is known about such diffusive dynamics in realistic dimensional spaces.

In order to go beyond the MFT, we study in this letter the dynamics of a simplest 'diffusing glass', namely directed polymer in random media (DPRM) [4] on a two dimensional square lattice by extensive MC simulations. The previous MC simulations [5,6] have found encouraging signatures of non-stationary dynamics under zero driving force but many open questions remained.

We find that the $k = 0$ component of current (velocity) correlation function and linear conductivity exhibit novel scaling behaviors which reveal 'one step' violations of the time translational invariance (TTI) and the Green-Kubo (GK) formula or the fluctuation dissipation theorem (FDT) for 'currents' [7]. On the other hand, finite k components equilibrate in the time $\tau_k \propto k^{-z(T)}$.

Model.— Our model is a lattice string on a two dimensional square lattice of size L in the longitudinal direction z and M in the transverse direction x . The string is directed in z direction and its segments are labeled as $x(z)$ ($z = 1, 2, \dots, L$). They obey the RSOS (Restricted Solids on Solid) condition, i.e. $|x(z) - x(z-1)| = 0, \pm 1$. Random potential $V(z, x)$ is defined on each lattice site (z, x) which takes a random value from the uniform distribution between -1 and 1. This system is known to be in the glassy phase at all finite temperatures. [4]

The dynamics is introduced by a heat-bath type MC method [5,6] which ensures that the microscopic motions of the *kinks* and *anti-kinks* are thermalized with the heat-

bath at a temperature T_{bath} . In one Monte Carlo Step (MCS), the whole configuration is swept once. The energy of the system at time t is given by

$$E(t)[V, h] = \sum_{z=1}^L V(z, x(z, t)) - h(z, t)x(z, t), \quad (1)$$

where $h(z, t)$ is the transverse force. As in the case of static properties [4], we assume that the dynamics of the present lattice model and the continuous model studied in the MFT have same asymptotic scaling properties.

We have performed simulations similar to the zero field cooling (ZFC) experiments of spin-glass systems. [2]. At first, a certain *waiting time* t_2 is elapsed under zero field starting from an out-of equilibrium initial configuration. Then a constant field $h(z')$ is applied at z' afterwards.

If linear response holds, the induced *current* at z , i. e. temporal transverse velocity of the segment $x(z)$, to be measured at time $t_1 (> t_2)$ can be written as,

$$\delta J_{z-z'}(t_1, t_2) = \int_{t_2}^{t_1} dt' \sigma_{z-z'}(t_1, t') h(z'), \quad (2)$$

where $\sigma_{z-z'}(t, t')$ ($t > t'$) is a time-dependent conductivity. Instead of the currents, we measure the linear susceptibility (induced displacement divided by h),

$$\begin{aligned} \chi_{z-z'}(t_1, t_2) &= \int_{t_2}^{t_1} dt \frac{\delta J_{z-z'}(t, t_2)}{h(z')} \\ &= \int_{t_2}^{t_1} dt \int_{t_2}^t dt' \sigma_{z-z'}(t, t'). \end{aligned} \quad (3)$$

Let us here introduce a generalized Green-Kubo (GK) formula,

$$\sigma_{z-z'}(t_1, t_2) = \frac{Y_{z-z'}(t_1, t_2)}{T_{\text{bath}}} < J_z(t_1) J_{z'}(t_2) > \theta(t_1 - t_2), \quad (4)$$

where $< J_z(t_1) J_{z'}(t_2) > \equiv \partial_{t_1} \partial_{t_2} < x(z, t_1) x(z', t_2) >$ is the current correlation function. The usual GK formula [7] corresponds to the case with the 'FDT ratio' $Y = 1$. Hereafter, the bracket $< \dots >$ means the average over

samples: different realizations of initial configurations, thermal histories (MC runs) and random potentials.

By integrating the current correlation function over the two time variables we obtain,

$$B_{z-z'}(t_1, t_2) \equiv \int_{t_2}^{t_1} dt \int_{t_2}^{t_1} dt' \langle J_z(t) J_{z'}(t') \rangle \\ = \langle [x(z, t_1) - x(z, t_2)][x(z', t_1) - x(z', t_2)] \rangle. \quad (5)$$

Combining with (3), the *integral* violation of the FDT can be defined as,

$$I_{z-z'}(t_1, t_2) = B_{z-z'}(t_1, t_2)/2 - T_{\text{bath}} \chi_{z-z'}(t_1, t_2). \quad (6)$$

We define the Fourier transform along z axis as $\chi_k(t_1, t_2) = \sum_{r=0}^L \cos(kr) \chi_r(t_1, t_2)$ and $B_k(t_1, t_2) = \sum_{r=0}^L \cos(kr) B_r(t_1, t_2)$ where $k = n\pi/L$ with ($n = 0, 1, \dots, L$). Note that $B_{k=0}$ is proportional to the mean-squared displacement of the center of mass.

In the following, we begin with the crossover between the linear and non-linear response. Then, we discuss aging effects in linear responses and correlation functions.

Crossover between linear and non-linear response.— As often emphasized, the non-linear effects due to the collective creep [3] should be dominant asymptotically. However one can systematically expel them out of a given time window by decreasing h because the characteristic time to create the nucleus of the creep diverges rapidly as h is decreased by the well known formula $\ln \tau_{\text{creep}} \propto h^{-\mu}$ with the glassy exponent $\mu = 1/4$ in two dimension. We demonstrate it in the following.

We have performed simulations of system size $L = 500$ $M = 520$, at temperature $T_{\text{bath}} = 0.4$ under *uniform* transverse fields. The periodic boundary condition is imposed on both x and z directions and straight lines are chosen as initial configurations.

In Fig. 1, we show data of the susceptibility $\chi_{k=0}(\tau, 0)$ at different strength of fields h in a double logarithmic plot. There are crossovers from the linear response curve where data of different h merge with each other to the non-linear branches which depart from the common curve. The non-linear branch grow linearly with τ by different velocities $v(h)$. In the inset of Fig. 1 we show the effective velocity $v(h)$ determined by fitting the non-linear branches to the form $h\chi(\tau, 0) = v(h)\tau + c(h)$ where $c(h)$ is a parameter. The result is consistent with the expected behavior $\ln v(h) \propto -\ln \tau_{\text{creep}}$. More details of the crossover phenomena will be reported elsewhere.

Aging Effects.— Let us begin discussions on aging effects in the linear susceptibility χ and integrated correlation function B at zero wavenumber $k = 0$.

In Fig. 2 we show the data of $\chi_{k=0}$ and $B_{k=0}$ of different waiting times t_2 against the time difference $\tau = t_1 - t_2$ in double logarithmic plots. The system size is $L = 500$ and temperature is $T_{\text{bath}} = 0.4$. We have checked that there are no finite size effects up to 10^6 MCS within the

statistical accuracy by simulating larger systems. We have chosen weak enough uniform field $h = 0.005$ in order to measure linear responses up to 10^6 MCS.

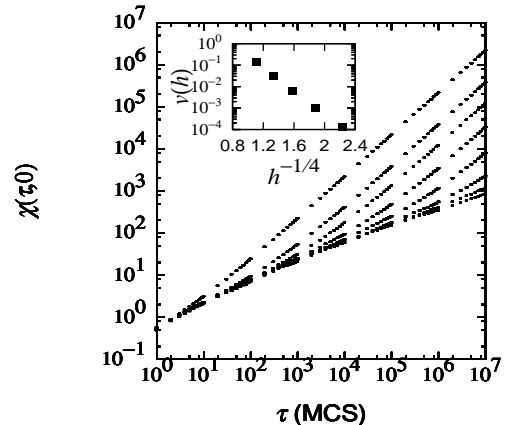


FIG. 1. Crossover between linear and non-linear responses. The strength of the uniform field is varied as $h = 0.64, 0.32, 0.16, 0.08, 0.04, 0.02, 0.01, 0.005, 0.0025$ from the top curve to the bottom. The error bars are of the size of the symbols. The average is took over 100 samples. (1000 samples for $h = 0.005$ and 0.0025) The inset is the velocity $v(h)$ versus $h^{-1/4}$ at $h = 0.64, 0.32, 0.16, 0.08, 0.04$.

Except the rapid growth at $\tau < 10^2$ MCS, which is discarded in the following as a short time transient behavior, the general feature is the following: each curve of a given waiting time t_2 follows initially the lower 'quasi-equilibrium' branch then switches over to the upper 'aging' branch at around $\log \tau \sim \log t_2$. Here the existence of aging effects is evident. Both χ and B violates TTI: they are not functions of the time difference $\tau \equiv t_1 - t_2$ alone but explicitly depends also on the *waiting time* t_2 .

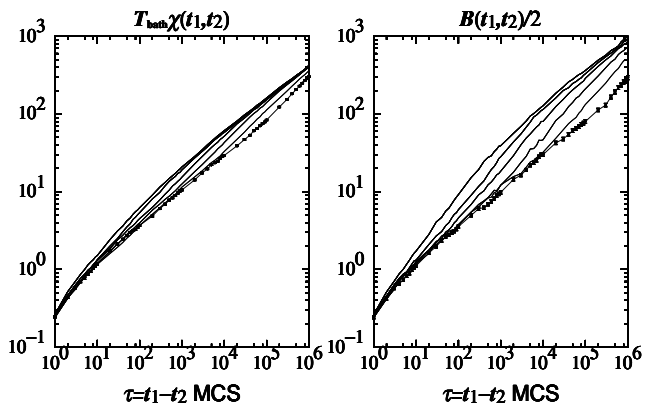


FIG. 2. $T_{\text{bath}} \chi_{k=0}(t_1, t_2)$ and $B_{k=0}(t_1, t_2)/2$ of waiting times $t_2 = 10, 10^2, 10^3, 10^4, 10^5, 10^6$ from the left curve to the right. Only lines connecting the data points at $\tau = t_1 - t_2 = n \times 10^p$ (where $n = 1, 2, \dots, 9$ and $p = 0, 1, \dots, 5$) are shown for graphical convenience. The average is took over 1050 samples. Typical sizes of the error bars are those of the symbols on the curve of $t_2 = 10^6$ (bottom).

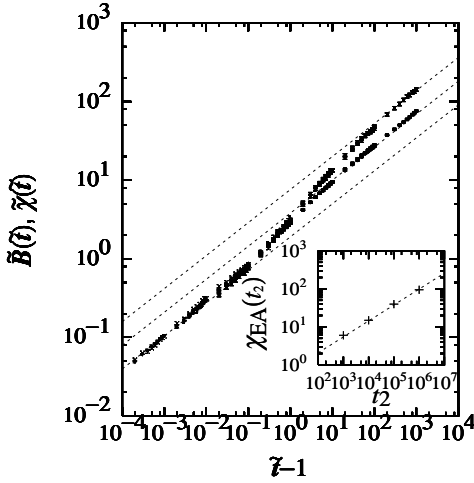


FIG. 3. Scaling plot of the susceptibility and the mean-squared displacement. (lower and upper curves respectively) The inset is the scaling parameter $\chi_{EA}(t_2)$ vs t_2 . We use the data of $\tau > 10^2$ (MCS) at $t_2 = 10^3, 10^4, 10^5, 10^6$ (MCS). All the broken lines are algebraic law fits of the same exponent $2/z(T_{\text{bath}} = 0.4) = 0.42$ with different amplitudes, from which we obtain $c_2/c_1 \simeq 4.0$ and $y \simeq 0.5$.

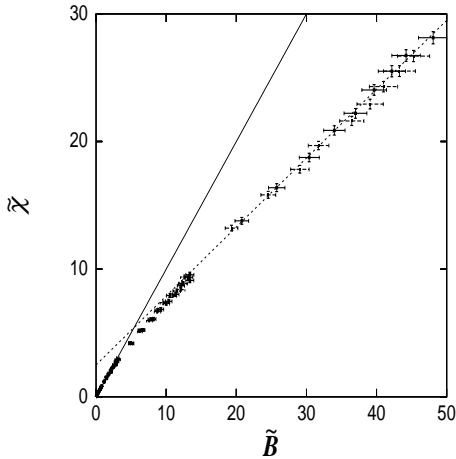


FIG. 4. Parametric plot of the scaling functions $\tilde{\chi}(\tilde{t})$ and $\tilde{B}(\tilde{t})$ shown in Fig. 3. The solid straight line represents the integrated FDT. The dashed line is a fit by a straight line with slope $y = 0.54$ to the part where the FDT is violated.

The *one step* structures can be well described by the following simple scaling ansatz:

$$\begin{aligned} T_{\text{bath}}\chi_{k=0}(t_1, t_2) &\simeq S_\chi(t_1/t_2)(t_1 - t_2)^{2/z(T)} \\ B_{k=0}(t_1, t_2)/2 &\simeq S_B(t_1/t_2)(t_1 - t_2)^{2/z(T)}. \end{aligned} \quad (7)$$

Here $S_\chi(\tilde{t})$, $S_B(\tilde{t})$ are step-like functions in the scaled time variable $\tilde{t} = t_1/t_2$. They take a) the same value c_1 in the 'quasi-equilibrium time domain' $\tilde{t} \ll 1$ and b) different values $yc_2 (> c_1)$ and $c_2 (> c_1)$ respectively in the 'aging time domain' $\tilde{t} \gg 1$. The ratio y is smaller than 1. The latter means that the integral violation of

FDT (6) exists : $I > 0$ in the 'aging time domain'.

In the absence of the random potential, the present model is equivalent to the free Gaussian field model [8] in which $z = 2$: the diffusion is 'normal'. Further more S_χ and S_B are constants (mobility or diffusion constant) and equal. Thus TTI and the FDT holds completely.

In order to test the scaling ansatz (7), we consider equivalent formulas: $T_{\text{bath}}\chi_{k=0}(t_1, t_2) \simeq \chi_{EA}(t_2)\tilde{\chi}(\tilde{t})$ and $B_{k=0}(t_1, t_2)/2 \simeq \chi_{EA}(t_2)\tilde{B}(\tilde{t})$ where $\chi_{EA}(t_2) = t_2^{2/z(T)}$ scales the 'height of step'. The scaling functions read as $\tilde{\chi}(\tilde{t}) = S_\chi(\tilde{t})|\tilde{t}-1|^{2/z(T)}$ and $\tilde{B}(\tilde{t}) = S_B(\tilde{t})|\tilde{t}-1|^{2/z(T)}$. We assume that $\tilde{t} = t_1/t_2$ is the correct scaling variable and treat $\chi_{EA}(t_2)$ as a scaling parameter [9] to be determined for each t_2 . The resultant master curves and the scaling parameters $\chi_{EA}(t_2)$ are shown in Fig. 3. In Fig. 4, we show a parametric plot of the master curves which clearly shows 'one step' violation of the FDT.

From (7), we can deduce scaling forms for the linear conductivity and correlation function of the current at $k = 0$. Except around the *step* $\log(t_1/t_2 - 1) \sim 0$, we find power laws multiplied by the 'one step' functions,

$$\begin{aligned} T_{\text{bath}}\sigma(t_1, t_2) &\simeq S_\chi(t_1/t_2)(t_1 - t_2)^{-2(1-1/z(T))} \\ \langle J(t_1)J(t_2) \rangle &\simeq S_B(t_1/t_2)(t_1 - t_2)^{-2(1-1/z(T))}. \end{aligned} \quad (8)$$

In the last equations we have used $\sigma(t_1, t_2) = -\partial_{t_1}\partial_{t_2}\chi(t_1, t_2)$, $\langle J(t_1)J(t_2) \rangle = -\partial_{t_1}\partial_{t_2}B(t_1, t_2)/2$ and omitted the common pre-factor $-2/z(T)(1-2/z(T))$. So both *noise* and *response* violate TTI and the FDT. The 'FDT ratio' $Y(t_1, t_2)$ (4) shows 'one step' variation : $Y = 1$ in the the 'quasi-equilibrium time domain' and $Y = y$ in the 'aging time domain'.

Let us now compare our results with the conventional picture based on the MFT [1]. There are now increasing number of numerical studies on different glassy systems such as a spin-glass model [10], Lennard-Jones Glasses [11], and coarsening in spin-systems [12], which appear to *roughly* support the picture based on similar dynamical MFTs [13]. However we find that the crucial concept of the MFTs [1,13] called as 'correlation scales' cannot be applied to our system as we discuss below.

The MFT assumes that TTI and the FDT hold in the quasi-equilibrium scale $B < B_{EA}$ but not in the aging scale $B > B_{EA}$. The border line between the two scales B_{EA} is a well-defined constant. Consequently, the correlation and response functions becomes the *sum* of the contributions from the quasi-equilibrium and aging scale.

However, the *multiplicative* scaling form (7) certainly disagree with the MFT. The 'height of step' $\chi_{EA}(t_2)$, which corresponds to the B_{EA} of the MFT, is *not* at all a constant but apparently increases with time t_2 as shown in the inset of Fig. 3 (similar effect has been noticed in the Sinai model [14]). Thus our results reveal considerable differences from the MFT. However, surprisingly, the 'one step' variation of the FDT ratio predicted by the MFT is recovered in an unexpected way.

Propagation of response.— Finally we discuss the propagation of responses along z axis. To this end, we have performed another set of simulations with *point* fields $h(z) = h_{\text{point}}\delta(z-L/2)$ which pull the center of the string $z = L/2$. We have obtained $\chi_r(t_1, t_2)$ by measuring the induced displacement of segments at various distance r from the center.

In Fig. 5. we show a set of data in a scaling plot in order to test the scaling law which holds in the pure system [8],

$$\chi_r(t_1, t_2) = \chi_{r=0}(t_1, t_2)H(r/\chi_{r=0}(t_1, t_2)). \quad (9)$$

Here $\chi_{r=0}(t_1, t_2)$ plays the role very similar to the 'domain size' in the *coarsening* systems [15]. In the scaling analysis, we have treated each $\chi_{r=0}(t_1, t_2)$ as a scaling parameter to be determined for each (t_1, t_2) .

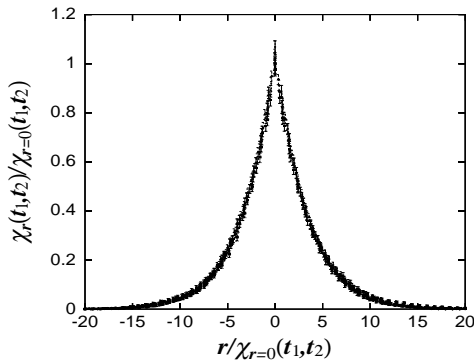


FIG. 5. Scaling plot of the profile $\chi_r(t_1, t_2)$ at $t_2 = 10^3, 10^4, 10^5, 10^6$ and $\tau = 10^3, 10^4, 10^5, 10^6$. The system size is $L = 500$ and temperature is $T_{\text{bath}} = 0.4$. The average is taken over 11520 samples. The non-linear effect is much weaker than in the case of uniform fields and we have used safely point field of strength $h_{\text{point}} = 0.1$ to investigate linear-response up to 10^6 MCS.

The resultant master curve $H(\tilde{r})$ drops linearly $H(\tilde{r}) = 1 - \tilde{r}$ at $\tilde{r} < 2$ and has a Gaussian tail at $\tilde{r} > 10$. Surprisingly, it is virtually indistinguishable from that obtained by simulating a corresponding pure system within our numerical accuracies.

In the Fourier space, the scaling form (9) takes the same form as in the MFT [1], $k^2\chi_k(t_1, t_2) = F(k^2\chi_{k=0}(t_1, t_2))$ where $\chi_{k=0}(t_1, t_2) = h\chi_{r=0}^2(t_1, t_2)$. (Our data satisfy latter within our numerical accuracies.) In the last equations we used $h \equiv \int_0^\infty dy H(y)$ and $F(x) \equiv (x/h) \int_0^\infty dy \cos(y\sqrt{x/h})H(y)$. Combining with (7) we find that 'domain size' grows as $\chi_{r=0}(t_1, t_2) \simeq \sqrt{S_\chi(t_1/t_2)/h}(t_1 - t_2)^{1/z(T)}$. In other words, a finite k component equilibrates in the time $\tau_k \propto k^{-z(T)}$ to the equilibrium value $\chi_k^{\text{eq}} \propto k^{-2}$. The latter k^{-2} scaling is due to the so called statistical tilt symmetry [16].

The exponent $z(T_{\text{bath}} = 0.4) \simeq 4.8$ is much larger than in the pure model $z = 2$. We have found that $z(T)$ increases with decreasing temperature. Though the previ-

ous work [5] proposed a logarithmic law for the susceptibility the present data of increased statistical accuracy over enlarged time range fit better to the algebraic law in (7). Thus the naive scaling argument based only on *typical* energy barrier [5] which suggest the logarithmic law should be inaccurate.

To summarize, we performed extensive MC simulations and scaling analysis on the aging effects of a 'diffusing glass', 2 dimensional DPRM. We found that the correlation and linear response functions exhibit interesting 'one-step' scaling phenomena. It will be very interesting if such features can be observed experimentally in some 'diffusing glasses', such as vortex lines in dirty type-II super-conductors.

The author gratefully thanks A. Barrat, J. P. Bouchaud, L. F. Cugliandolo, M. Hamman, J. Kurchan, H. Rieger and H. Takayama for discussions and suggestions. This work was supported by Grand-in-Aid for Scientific Research from the Ministry of Education, Science and Culture, Japan. The computation has been done using the facilities of the Supercomputer Center, ISSP, the Univ. of Tokyo, the Computer Center, the Univ. of Tokyo and the Computer Center, Kyushu University.

-
- [1] L. F. Cugliandolo and P. Le Doussal, Phys. Rev. E **53** 1525 (1996), Cugliandolo, J. Kurchan, and P. Le Doussal, Phys. Rev. Lett. **76**,2390 (1996).
 - [2] Lundgren L., Svedlindh P., Nordblad P. and Beckmann O., Phys. Rev. Lett. 1983 **51** 911; E. Vincent, J. Hammann and M. Ocio, in *Recent Progress in Random Magnets* (World Scientific, Singapore, 1992)
 - [3] G. Blatter, M. V. Feigel'man V. B. Genkenbein, A. I. Larkin and V. M. Vinokur, Rev. Mod. Phys. vol 66 1125 (1994).
 - [4] T. Halpin-Healy and Y.C. Zhang, Phys. Rep. **254**, 215 (1995).
 - [5] H. Yoshino, J. of Phys. **A29**, 1421 (1996).
 - [6] A. Barrat, Phys. Rev. E **55**, 5651 (1997).
 - [7] R. Kubo, M. Toda and N. Hashitume; *Statistical Mechanics II. Nonequilibrium Statistical Mechanics 2nd. Edition*, (Springer-Verlag, 1992).
 - [8] L. F. Cugliandolo, J. Kurchan and G. Parisi, J. Physique I (France) **4**, 1641 (1994).
 - [9] L. F. Cugliandolo and J. Kurchan (private communication).
 - [10] S. Franz and H. Rieger, J. Stat. Phys. **79**, 749 (1995).
 - [11] G. Parisi, Phys. Rev. Lett. **79**, 3660 (1997).
 - [12] A. Barrat, Phys. Rev. **E 57**, 3629 (1998).
 - [13] J. P. Bouchaud, L. F. Cugliandolo, J. Kurchan and M. Mézard in *Spin-glasses and random fields*, edited by A. P. Young, (World Scientific, Singapore, 1997).
 - [14] L. Laloux and P. L. Doussal, Phys. Rev. **E 57**, 6296 (1998).
 - [15] A. J. Bray, Adv. Phys. **43**, 357 (1994).
 - [16] T. Hwa and D.S. Fisher, Phys. Rev. **B 49**, 3136 (1994).